

$S_1 \leftarrow S_0$ Vibronic spectrum and structure of fluoral in the S_1 state

I. A. Godunov,* N. N. Yakovlev, and E. B. Averina

Department of Chemistry, M. V. Lomonosov Moscow State University,
Leninskie Gory, 119899 Moscow, Russian Federation.

Fax: +7 (095) 932 8846.

E-mail: godunov@molesp.chem.msu.su

The vibronic absorption spectrum of fluoral vapor was studied in the region of the $S_1 \leftarrow S_0$ electronic transition (313–360 nm). The origin (0_0^{0+}) of the transition (29419 cm^{-1}) and a number of fundamental frequencies in the S_0 and S_1 states were determined. The character of intensity distribution in the spectral bands indicates that the electronic excitation leads to significant change of the CF_3 group orientation relative to the molecular frame. Moreover, it was found that the carbonyl fragment of the molecule in the S_1 state has pyramidal structure (in contrast, the carbonyl fragment of the fluoral molecule in the S_0 state is planar). The experimental torsion and inversion energy levels were used for the calculation of internal rotation and inversion potential functions of fluoral molecule in the S_1 state. The potential barriers to internal rotation and inversion were found to be 1270 cm^{-1} (15.2 kJ mol^{-1}) and 550 cm^{-1} (6.6 kJ mol^{-1}), respectively. The conformational changes caused by $S_1 \leftarrow S_0$ electronic excitation in the fluoral molecule are similar to those observed in acetaldehyde and biacetyl molecules and differ from the conformational behavior of hexafluorobiacetyl molecule.

Key words: vibronic spectrum, structure, excited electronic state, fluoral, fundamental frequencies, potential functions, internal rotation, inversion.

Analyzing our own and literature experimental data, we established previously¹ several features of the structure of carbonyl compounds in the ground (S_0) and lowest excited singlet (S_1) and triplet (T_1) electronic states. In particular, it was noted that the $S_1 \leftarrow S_0$ electronic excitation of acetaldehyde (CH_3COH), methylglyoxal (CH_3COCO), and biacetyl ($\text{CH}_3\text{COCOCH}_3$) molecules leads to the rotation of methyl groups relative to the molecular frame as well as to the pyramidal distortion of the carbonyl fragments from the planar geometry pertinent to the molecules in the S_0 electronic states. In contrast, the $S_1 \leftarrow S_0$ excitation of hexafluorobiacetyl molecule ($\text{CF}_3\text{COCOCH}_3$) leads neither to the CF_3 group rotation, nor to the pyramidal distortion of the carbonyl fragments.¹ It is interesting in this respect to study the conformational behavior of the fluoral molecule (CF_3COH) upon the electronic excitation to the lowest excited T_1 and S_1 states.

Since the structure of fluoral molecule in the S_1 and T_1 states had not been studied previously, we obtained and analyzed the vibronic spectrum of the fluoral molecule in the regions of $S_1 \leftarrow S_0$ and $T_1 \leftarrow S_0$ electronic transitions. The results of $S_1 \leftarrow S_0$ vibronic spectrum analysis are presented below, whereas the study of $T_1 \leftarrow S_0$ transition will be presented elsewhere.²

The structure and spectral properties of the fluoral molecule in the S_0 state were studied in sufficient detail. The geometric parameters of the molecule were determined by means of gas-phase electron diffraction.³ The microwave spectroscopic studies^{4,5} made it possible to estimate the height of the barrier to internal rotation as 309 and 305 cm^{-1} (3.70 and 3.65 kJ mol^{-1}), respectively.

Complete assignment of the fundamental frequencies in the vibrational spectra of fluoral molecule was carried out^{4,7–12} and the energies of the three lowest torsion levels were determined. From these data the height of the potential barrier to internal rotation was calculated¹¹ as 292 cm^{-1} (3.45 kJ mol^{-1}).

Low-resolution UV absorption spectrum of the fluoral vapor in the 10-cm cell in the 200–400 nm region was also recorded previously.¹² The absorption band at 230–360 nm with the intensity maximum at 300 nm was assigned¹² to the $S_1 \leftarrow S_0$ ($n \rightarrow \pi^*$) electronic transition typical of carbonyl molecules. Its origin was roughly estimated as ~350 nm. Weak absorption at the long-wave spectral region was also observed.

In addition, *ab initio* calculations on the geometry, normal mode frequencies and intensities of the fluoral molecules in the S_0 state were performed.^{12,13} The height of the potential barrier to internal rotation was

estimated as 3.47 kJ mol⁻¹. In agreement with experimental data, the results of these calculations indicate that in the equilibrium configuration of the fluoral molecule the O atom eclipses the F atom. It is worth noting that determination of the geometric parameters of the fluoral molecule from the microwave spectra is complicated because the F atoms cannot be replaced by other isotopes and, in addition, O and C atoms lie almost along the principal axis of inertia.⁵

Experimental

Fluoral was synthesized by the reduction of trifluoroacetic acid by lithium hydride.¹⁴ The IR spectrum of the prepared sample completely coincided with the literature spectrum⁴ within the 400–4000 cm⁻¹ frequency range.

UV absorption spectrum of the fluoral vapor in the 310–400 nm range was recorded photographically using the DFS-452 spectrograph with a first-order diffraction grating of 2400 lines mm⁻¹ and a theoretical resolving power 120000. A multi-pass cell with optical path length from 10 to 200 m operating under vapor pressures from 1 to 300 Torr was implemented.

The spectrum of a hollow Fe–Ne-cathode lamp was accepted as the reference. The positions of lines were measured by means of an IZA-2 comparator.

The spectrum obtained has rich vibrational structure in the 32000–25400 cm⁻¹ (313–394 nm) range. The spectral patterns in the high-frequency 32000–27800 cm⁻¹ (313–360 nm) range significantly differ from those in the low-frequency 28800–25400 cm⁻¹ (347–394 nm) one. Moreover, the low-frequency part of the spectrum is generally much less intense than its high-frequency part even though it is recorded at the maximum optical path length and the pressure of the fluoral vapor. We assigned the vibronic spectra of the fluoral molecule in the 32000–27800 cm⁻¹ and 28800–25400 cm⁻¹ ranges to the S₁←S₀ and T₁←S₀ electronic transitions, respectively, in agreement with the data on the other carbonyl compounds¹

and on the fluoral molecule obtained in Ref. 12 cited above. The results of vibrational analysis of the S₁←S₀ electronic transition will be presented below. The vibronic spectrum of the fluoral molecule in the 347–394 nm range will be considered elsewhere.²

Results and Discussion

Within the 32000–27800 cm⁻¹ range more than ten similar groups of bands were observed. Most of the groups consist of sequences of pairs of bands with spacing between the bands in a pair ~40 cm⁻¹. The intensity of the pairs of bands increases and passes through the maximum within each group (Fig. 1). Taking into account the intervals between the low-frequency components of each pair and their intensity distributions, it is reasonable to assign their low-frequency components to the torsion transitions. Similar characteristic groups of bands were observed in the S₁←S₀ spectra of the related carbonyl molecules like acetaldehyde,¹⁵ *cis*- and *gauche*-propanal conformers,^{16,17} *trans*- and *gauche*-2-methylpropanal conformers,¹⁸ and 2,2-dimethylpropanal.¹⁹ In particular, pairs of bands with 33–48 cm⁻¹ spacing between the components appear in the spectra of all these molecules as a result of inversion splitting of the zero-point vibrational levels of the molecules in the S₁ state. Similarly, the bands of the characteristic groups in the S₁←S₀ fluoral spectrum can be also assigned to the torsion-inversion transitions (Table 1). The wave numbers and assignments of pseudoorigins of the characteristic groups of bands are listed in Table 2.

According to our assignment, the origin of the S₁←S₀ electronic transitions, i.e., the 0₀⁰ transition between the zero-point levels of the S₀ and S₁ states corresponds

Table 1. Wave numbers (ω/cm⁻¹) and assignment of the band groups of the S₁←S₀ vibronic spectrum of the fluoral molecule in the region of the 0₀⁰ transition

Band	ω _i	Intensity	Δω _i	Assignment	Band	ω _i	Intensity	Δω _i	Assignment
1	29292	m*	-127	12 ₀ ⁰ +15 ₂ ⁰	2	29332	w	-87	12 ₀ ⁰ -15 ₂ ⁰
3	29355	s	-64	12 ₀ ⁰ +15 ₁ ⁰	4	29396	w	-23	12 ₀ ⁰ -15 ₁ ⁰
5	29419	w	0	12 ₀ ⁰ +(0 ₀ ⁰)	6	29460	v.w	41	12 ₀ ⁰ -(0 ₀ ⁰)
7	29484	w, b	65	12 ₀ ⁰ +15 ₁ ¹	8	29520	v.w	101	12 ₀ ⁰ -15 ₁ ¹
9	29545	w	126	12 ₀ ⁰ +15 ₀ ¹	10	—	—	—	—
11	29602	s	183	12 ₀ ⁰ +15 ₁ ²	12	29640	m	221	12 ₀ ⁰ -15 ₁ ²
13	29670	v.s	251	12 ₀ ⁰ +15 ₀ ²	14	29710	s	291	12 ₀ ⁰ -15 ₀ ²
15	29730	m	311	12 ₀ ⁰ +15 ₁ ³	16	29762	w	343	12 ₀ ⁰ -15 ₁ ³
17	29795	m	376	12 ₀ ⁰ +15 ₀ ³	18	—	—	—	—
19	29840	m	421	12 ₀ ⁰ +15 ₁ ⁴	20	—	—	—	—

Note. Hereafter the standard notations for vibronic transitions $N_{\nu''}\nu'$ are used, where N is the number of vibration, ν'' and ν' are the vibrational quantum numbers for the ground and excited electronic states: $N = 12$ and 15 correspond to inversion and torsion vibrations, respectively; 0₀⁰ refers to the transition between the zero-point vibrational levels of the ground and excited electronic states; the signs + and - denote upper and lower (in energy) components of inversion splitting for the levels of the S₁ state; intensities are characterized as v.s is very strong, s is strong, m is medium, w is weak, and v.w is very weak; b indicates broad bands.

* The band coincides with the band of the 12₄⁴+15₁⁴ transition.

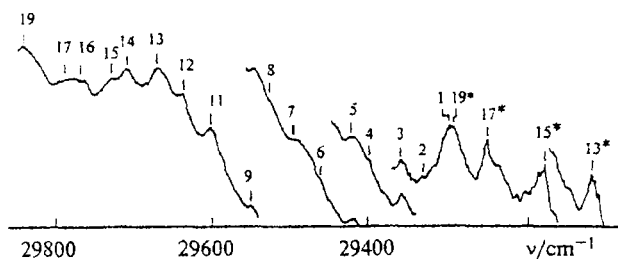


Fig. 1. Microdensitometer trace showing the part of the S₁←S₀ vibronic spectrum of the fluoral molecule in the region of the 0₀⁰ transition. The vibronic bands 1–19 are listed in Table 1; the bands with the number and asterisk correspond to the 12₄⁴⁺15₅⁵ transitions (see text).

to the 29419 cm^{−1} band. This assignment is confirmed by the observation of the group of intensive torsion transition bands with the pseudoorigin at 1189 cm^{−1} pertinent to the molecules of other carbonyl compounds¹ and corresponding to the valence vibrational frequency ν₂(C=O) of the fluoral molecule in the S₁ state.

The pseudoorigins at 449 and 765 cm^{−1} accompanied by the characteristic groups of the single bands (rather than of their pairs) correspond therefore to the transitions to high inversion levels of the S₁ state of the fluoral molecule.

The pseudoorigin at 248 cm^{−1} can be assigned to the frequency of the planar deformation vibration ν₉[′] (CCO) in the S₁ state. Indeed, in the S₀ state¹⁰ ν₉[′] = 430

cm^{−1} so the frequency ratio ν₉[′]/ν₉[′] = 0.58 almost coincides with the corresponding value 321 cm^{−1}/587 cm^{−1} = 0.55 determined previously for the 2,2-dimethylpropanal¹⁹ molecule.

We assigned the pseudoorigins at 590 and 810 cm^{−1} to the frequencies of symmetric deformation ν₇[′] (CF₃) and valence ν₆[′] (C–C) vibrations, respectively. In the S₀ state¹⁰ ν₇[′] = 705 cm^{−1} and ν₆[′] = 840 cm^{−1}.

In addition, combinations of the above-mentioned frequencies and four pseudoorigins at −554, −1514, −590, and −1546 cm^{−1} corresponding to the hot transitions were observed in the spectrum. The differences between the first two and the second two pseudoorigins (960 and 956 cm^{−1}) coincide with the frequency of non-planar CH vibration (ν₁₂[′]) of the molecule in the S₀ state¹⁰ (958 cm^{−1}). The pseudoorigins at −590 and −1546 cm^{−1} are accompanied by pairs of torsion-inversion bands (with 40 cm^{−1} spacing within a pair), whereas the pseudoorigins at −554 and −1514 cm^{−1} give rise to groups of single intense torsion transition bands (see Fig. 1). Hence, the pseudoorigins at −554 and −1514 cm^{−1} are connected with the hot transitions to high inversion levels of the S₁ state (see Table 2). Their assignments will be discussed below. We assigned the pseudoorigins at −590 and −1546 cm^{−1} to the transitions related to the frequency of planar CH vibration in the S₁ state (ν₃[′]), see Table 2.

The assignments of vibronic bands presented in the Tables 1 and 2 as well as their intensity distribution indicate that the S₁←S₀ electronic excitation of the fluoral molecule leads to the rotation of the −CF₃ group with respect to the molecular frame and to the pyrami-

Table 2. Wave numbers (ω_i/cm^{−1}) and assignments of pseudoorigins in the S₁←S₀ spectrum and vibrational frequencies (ν_i) of the fluoral molecule in the S₁ and S₀ states

ω _i	Inten- sity	Δω _i	Assign- ment	ν _i		
				symmetry and form	S ₁	S ₀ ¹⁰
28124	v.w	−1546	3 ₀ ¹ 12 ₃ ⁰⁺ 15 ₀ ²	ν ₂ (C=O str., a′)	1189	1737
28156	v.w	−1514	12 ₄ ⁴⁺ 15 ₀ ²	ν ₃ (CH bend., a′)	1326	1387
29080	w	−590	3 ₀ ¹ 12 ₂ ⁰⁺ 15 ₀ ²	ν ₆ (C–C str., a′)	810	840
29116	v.s	−554	12 ₄ ⁴⁺ 15 ₀ ²	ν ₇ (CF ₃ bend., a′)	590	705
29670	v.s	0	12 ₀ ⁰⁺ 15 ₀ ²	ν ₉ (CCO bend., a′)	248	430
29710	v.s	40	12 ₀ ⁰ −15 ₀ ²	ν ₁₂ (invers., a′)	40 *	958
29918	m	248	9 ₀ ¹ 12 ₀ ⁰⁺ 15 ₀ ²			
30119	m	449	12 ₀ ¹⁺ 15 ₀ ²			
30260	m	590	7 ₀ ¹ 12 ₀ ⁰⁺ 15 ₀ ²			
30435	m	765	12 ₀ ¹ −15 ₀ ²			
30480	s	810	6 ₀ ¹ 12 ₀ ⁰⁺ 15 ₀ ²			
30859	v.s	1189	2 ₀ ¹ 12 ₀ ⁰⁺ 15 ₀ ²			
31108	w, b	1438	2 ₀ ¹ 9 ₀ ¹ 12 ₀ ⁰⁺ 15 ₀ ²			
31310	v.w, b	1640	2 ₀ ¹ 12 ₀ ¹⁺ 15 ₀ ²			
31447	v.w, b	1777	2 ₀ ¹ 7 ₀ ¹ 12 ₀ ⁰⁺ 15 ₀ ²			
31669	v.w, b	1999	2 ₀ ¹ 6 ₀ ¹ 12 ₀ ⁰⁺ 15 ₀ ²			

Note. The intervals Δω_i were measured between the bands corresponding to the 15₀² transitions since they are more intense in the groups, whereas the true pseudoorigins have weak intensity as a rule and are often masked by the stronger bands belonging to other groups; str. is stretching, bend. is bending, invers. is inversion vibrations.

* Inversion splitting of the zero-point vibrational energy level.

dal distortion of the carbonyl fragment. The measured data allowed us to determine the potential functions of inversion and internal rotation of the fluoral molecule in the S_1 state.

In the one-dimensional approximation, the inversion of the non-planar carbonyl fragment of the fluoral molecule in the S_1 state can be described by the Hamiltonian²⁰

$$\hat{H}(x) = -\frac{1}{2} \frac{d}{dx} g(x) \frac{d}{dx} + V(x), \quad (1)$$

where x is the inversion coordinate which can be approximately represented as the displacement of the C—H bond from the CCO plane by the angle θ

$$x = r(C-H) \cdot \theta. \quad (2)$$

The $g(x)$ function can be calculated approximately from the geometric parameters of the molecule and the nuclear masses.²⁰ In order to estimate the geometric parameters of the fluoral molecule in the S_1 state, we performed a rotational contour simulation for the vibronic bands using a program similar to that described previously.²¹ Vibronic bands of the $S_1 \leftarrow S_0$ transitions in the fluoral molecule look like broad ordinary peaks, which provide little information for the determination of the geometric parameters for the molecule in the S_1 state (see Fig. 1). Nevertheless, using the structural data for the fluoral molecule in the S_0 state published previously³ [$r(C=O) = 1.204$ Å, $r(C-C) = 1.540$ Å, $r(C-F) = 1.332$ Å, $r(C-H) = 1.090$ Å, angles $C-C-F = 110.2^\circ$, $C-C-O = 121.8^\circ$, and $C-C-H = 120^\circ$], we estimated the changes in the geometric parameters of the fluoral molecule upon $S_1 \leftarrow S_0$ excitation for the $r(CO)$ distance as $+0.13$ Å and for the $C-C-O$ angle as -5° . However, it was not possible to apply this method for estimating the equilibrium value of the CH bond displacement angle from the CCO plane because the displacements of light hydrogen atom cause too small a variation of the rotational constants of the molecule. The values obtained agree with the results of our *ab initio* quantum-

chemical calculations (their results will be published elsewhere).

The $g(x)$ function in the kinetic energy operator represents the inverse reduced mass. It was determined as the diagonal element of the g_{44} block of the kinetic energy matrix $G(4 \times 4)$ in the momentum representation, where three coordinates correspond to the overall rotation of the molecule whereas the fourth coordinate corresponds to the inversion (*i.e.*, the interaction of inversion with rotational motion was taken into account). In the calculations I and III (see Table 3) g_{44} was kept fixed, while in the calculations II and IV the change of g_{44} due to inversion was accounted for by means of the dependence

$$g(x) = \sum_{n=0}^8 g_n x^n. \quad (3)$$

Two model functions were used for approximating the inversion potential function

$$V(x) = V_2 x^2 + V_4 x^4 \quad (4)$$

(calculations I and II, Table 3) and

$$V(x) = V_2 x^2 + V_g \exp(-Px^2) \quad (5)$$

(calculations III and IV, Table 3).

At the first stage, only the energies of the 0^- , 1^+ and 1^- inversion levels were used for determination of the inversion potential function of the fluoral molecule in the S_1 state (see Table 2). The energies of higher inversion levels calculated with the resulting potentials made it possible to assign unambiguously the pseudorigin at -554 cm^{-1} to the hot transition $12_4^{4+} 15_0^{0-}$ (see Table 2). In the final calculations the experimental energy of the 4^+ inversion level was also included.

Table 4 lists the energies of inversion levels obtained from the experimental spectrum and theoretical calculations I–IV. As follows from the data presented in Tables 3 and 4, the results of the inversion potential function calculations I–IV for the fluoral molecule in the S_1 state agree well with each other.

Table 3. The heights of the inversion potential barrier $V(0)$ and equilibrium values of the C—H bond displacement angle from the CCO plane (θ_{\min}) for the fluoral molecule in the S_1 state from calculations I–IV

Calculations (equation)	θ_{\min} /deg	$V(0)$ /cm ⁻¹	V_2 /cm ⁻¹ Å ⁻²	V_4 /cm ⁻¹ Å ⁻⁴	V_g /cm ⁻¹	P Å ⁻²
I (4)	30	563	3585.6	5706.2	—	—
II (4)	29	562	3594.7	5747.9	—	—
III (5)	29	547	25995.8	—	65018.8	0.458
IV (5)	29	547	27501.9	—	71893.5	0.435

Note. Here and in Table 4 for the calculations I and III: $g_{44} = 1.049$ amu⁻¹, for calculations II and IV: $g_{44}(x) = g_0 + g_2 x^2 + g_4 x^4 + g_6 x^6 + g_8 x^8$; $g_0 = 1.049$ amu⁻¹; $g_2 = 1.461 \cdot 10^{-2}$ amu⁻¹ Å⁻²; $g_4 = 2.381 \cdot 10^{-3}$ amu⁻¹ Å⁻⁴; $g_6 = -2.135 \cdot 10^{-4}$ amu⁻¹ Å⁻⁶; $g_8 = 8.944 \cdot 10^{-6}$ amu⁻¹ Å⁻⁸.

Then the energies of torsion levels (see Table 1) were used for determination of the torsion potential function. Under the one-dimensional approximation, this motion can be described by the Hamiltonian

$$\hat{H}(\varphi) = -\frac{d}{d\varphi} F(\varphi) \frac{d}{d\varphi} + V(\varphi), \quad (6)$$

where φ is the angle of internal rotation. The rotational constant

$$F = h/8\pi^2 c I_{\text{red}}, \quad (7)$$

(where I_{red} is the reduced moment of inertia) was calculated from the geometric parameters of the fluoral molecule in the S₁ state determined in the rotational contour simulations as described above. For the equilibrium value of the C—H bond displacement angle from the CCO plane the value of 29° which corresponds to the minimum of inversion potential was assumed (see Table 3). The internal rotation potential function was taken in the form

$$V(\varphi) = \frac{1}{2} V_3 (1 - \cos 3\varphi) \quad (8)$$

Table 5 presents the F and V_3 values as well as the energies of torsion levels of the fluoral molecule in the S₁ state determined experimentally and calculated using the procedure described in Ref. 22. It is clear that the height of the potential barrier to internal rotation of the fluoral molecule in the S₁ state significantly exceeds that in the S₀ state^{4,5,11} (300 cm⁻¹).

Table 4. Measured and calculated energies (E) of inversion levels of the fluoral molecule in the S₁ state

Le- vel	E/cm^{-1}				
	Experi- ment	Calculations			
		I	II	III	IV
0 ⁻	40.0	41.7	42.0	46.8	46.8
1 ⁺	449.0	448.4	448.5	453.5	453.5
1 ⁻	765.0	747.8	748.5	760.4	760.4
4 ⁺	3278.0	3281.9	3281.8	3278.3	3278.3

Table 5. The values of rotational constant F (7), height of internal rotation barrier V_3 (8), and experimental and calculated energies of torsion levels of the fluoral molecule in the S₁ state

Level	E/cm^{-1}		Parameter
	Experiment	Calculation	
15 ¹	126.0	127.5	$F=1.502$
15 ²	251.0	251.4	$V_3=1270$
15 ³	376.0	371.6	
15 ⁴	485.0	487.7	

Therefore, the study of the vibronic spectrum of the fluoral molecule reveals that the S₁←S₀ electronic excitation induces significant changes in the structure of this molecule, *i.e.*, the orientation of the —CF₃ group relative to the molecular frame is changed, the height of the internal rotation potential barrier increases from 300 to 1270 cm⁻¹ (from 3.6 to 15.2 kJ mol⁻¹), the carbonyl fragment acquires non-planar structure, and the height of the inversion potential barrier becomes equal to 550 cm⁻¹ (6.6 kJ mol⁻¹). The conformational behavior of the fluoral molecule under S₁←S₀ electronic excitation is similar to those of acetaldehyde and biacetyl molecules and strongly differs from that of hexafluorobiacetyl one where S₁←S₀ excitation leads neither to the rotation of —CF₃ group nor to the pyramidal distortion of carbonyl fragments.¹

The reasons for the specific conformational behavior of the hexafluorobiacetyl molecule are still unclear. To understand them it is necessary to perform additional experimental studies of the spectra and structure of related carbonyl compounds, first of all, of the trifluoromethylglyoxal and trifluorobiacetyl molecules, as well as to implement the *ab initio* quantum-chemical methods for studying R₁COCOR₂ (R₁, R₂ = H, CH₃, CF₃) molecules in the ground and excited electronic states.

Such calculations must be performed at the advanced level in order to reproduce the conformational features of the molecules (*i.e.*, stable conformations, heights of internal rotation and inversion potential barriers) determined experimentally. Perhaps, analysis of the variations in electronic density distribution and the effects of intermolecular forces under electronic excitation will allow one to find an explanation to the observed conformational behavior.

References

1. I. A. Godunov and N. N. Yakovlev, *Zh. Struct. Khim.*, 1995, **36**, 269 [*Russ. J. Struct. Chem.*, 1995, **36**, 238 (Engl. Transl.)].
2. I. A. Godunov and N. N. Yakovlev, *Zh. Fiz. Khim.*, 1998, **72** [*Russ. J. Phys. Chem.*, 1998, **72** (Engl. Transl.)].
3. R. H. Schwendeman, Ph. D. Thesis, University of Michigan, 1956.
4. C. V. Berney, *Spectrochim. Acta*, Ser. A, 1969, **25**, 793.
5. R. C. Woods, *J. Chem. Phys.*, 1967, **46**, 4789.
6. D. W. Knight and A. P. Cox, *Chem. Phys. Lett.*, 1986, **132**, 103.
7. R. E. Dodd, H. L. Roberts, and L. A. Woodward, *J. Chem. Soc.*, 1957, 2783.
8. G. Hagen, *Acta Chem. Scand.*, 1971, **25**, 813.
9. J. R. Durig and W. J. Natter, *J. Raman Spectr.*, 1981, **11**, 32.
10. J. R. Durig, G. A. Guirgis, and B. J. Van der Veken, *J. Raman Spectr.*, 1987, **18**, 549.
11. J. R. Durig, A. R. Fanning, T. G. Sheehan, and G. A. Guirgis, *Spectrochim. Acta*, Ser. A, 1991, **47**, 279.
12. J. S. Francisco and I. H. Williams, *Mol. Physics*, 1992, **76**, 1433.

13. E. Ottavianielli, E. A. Castro, and A. H. Jubert, *J. Mol. Struct.*, 1992, **254**, 279.
14. M. Braid, H. Iserson, and F. E. Lawlor, *J. Am. Chem. Soc.*, 1954, **76**, 4027.
15. M. Noble and E. K. C. Lee, *J. Chem. Phys.*, 1984, **81**, 1632.
16. V. N. Alekseev and I. A. Godunov, *Zh. Fiz. Khim.*, 1993, **67**, 99 [*Russ. J. Phys. Chem.*, 1993, **67**, 89 (Engl. Transl.)].
17. V. N. Alekseev and I. A. Godunov, *Zh. Fiz. Khim.*, 1993, **67**, 498 [*Russ. J. Phys. Chem.*, 1993, **67**, 448 (Engl. Transl.)].
18. M. Badavi and I. A. Godunov, *Zh. Fiz. Khim.*, 1993, **67**, 490 [*Russ. J. Phys. Chem.*, 1993, **67**, 441 (Engl. Transl.)].
19. N. N. Yakovlev and I. A. Godunov, *Zh. Fiz. Khim.*, 1993, **67**, 1826 [*Russ. J. Phys. Chem.*, 1993, **67**, 1639 (Engl. Transl.)].
20. T. Ueda and T. Shimanouchi, *J. Chem. Phys.*, 1967, **47**, 4042.
21. J. C. D. Brand, *MTP International Review of Science. Ser. I, Phys. Chem.*, Vol. 3, Spectroscopy, Ed. by D. A. Ramsay, 1972, 155.
22. A. V. Abramnikov, *Zh. Fiz. Khim.*, 1995, **69**, 1048 [*Russ. J. Phys. Chem.*, 1995, **69**, 948 (Engl. Transl.)].

Received July 24, 1997